

A Ring-Shaped Tri-Axial Force Sensor for Minimally Invasive Surgery

Beibei Han, Yong-Jin Yoon, Muhammad Hamidullah, Angel Tsu-Hui Lin, and Woo-Tae Park

Abstract—This paper presents the design of a ring-shaped tri-axial force sensor that can be incorporated into the tip of a guidewire for use in minimally invasive surgery (MIS). The designed sensor comprises a ring-shaped structure located at the center of four cantilever beams. The ring design allows surgical tools to be easily passed through which largely simplified the integration process. Silicon nanowires (SiNWs) are used as piezoresistive sensing elements embedded on the four cantilevers of the sensor to detect the resistance change caused by the applied load. An integration scheme with new designed guidewire tip structure having two coils at the distal end is presented. Finite element modeling has been employed in the sensor design to find the maximum stress location in order to put the SiNWs at the high stress regions to obtain maximum output. A maximum applicable force of 5 mN is found from modeling. The interaction mechanism between the designed sensor and a steel wire has been modeled by FEM. A linear relationship between the applied load on the steel wire and the induced stress on the SiNWs were observed.

Keywords—Triaxial MEMS force sensor, Ring shape, Silicon Nanowire, Minimally invasive surgery.

I. INTRODUCTION

MINIMALLY Invasive Surgery (MIS) has been widely practiced in hospital over the last century because of its numerous advantages over traditional open surgery, such as reduced postoperative pain, shorter hospital stays and periods of disability, which is cost-effective for both hospitals and patients [1]. However, despite rapid development of MIS techniques it was still limited by a number of unsolved problems among which the lack of force feedback is crucial. Similarly, in the catheterization procedures, such as cardiovascular and thoracic interventional procedures, which are performed in a minimally invasive manner to treat tissues and organs by employing catheters and guidewires, the need of force sensation are particularly important as the surgeons totally lost the force sensation while the guidewire/catheter is interacting with blood vessels or tissues. Sometimes the blockage of the vessel lumen makes the operation even more challengeable.

Beibei Han, Muhammad Hamidullah and Angel Lin Tsu-Hui, are with the Institute of Microelectronics, The Agency for Science, Technology and Research (A*STAR), 11 Science Park Road, Singapore 117685 (phone: +65-93906297; E-mail: bhan1@e.ntu.edu.sg, muhammad@ime.a-star.edu.sg, linta@ime.a-star.edu.sg).

Beibei Han and Yong-Jin Yoon are with School of Mechanical & Aerospace Engineering, Nanyang Technological University, 50 Nanyang Avenue, Singapore 639798 (E-mail: yongjiny@ntu.edu.sg).

Woo-Tae Park is with Department of Mechanical and Automotive Engineering, Seoul National University of Science and Technology, Seoul, Korea. (E-mail: wtpark@seoultech.ac.kr).

So far the surgeons perform the catheterization procedures mainly with the assist of imaging techniques, such as X-ray fluoroscopy and Magnetic Resonance Imaging (MRI) to visualize the anatomy of patient and tract the guidewire/catheter. However, as an essential tool used in the catheterization procedures, the X-ray fluoroscope has obvious drawbacks such as poor soft tissue visualization and exposure to radiation which is harmful to both patients and physicians [2]. To overcome these disadvantages, the MRI technique was developed with excellent visual information and lessens the radiation dose [3]. However, these techniques could not provide sufficient information to detect the interaction between soft tissue and guidewire/catheter. In order to detect the tool-tissue interaction and avoid imposing extra force, force sensors can be mounted on the surgical tools during the interventional procedures. Microelectromechanical systems (MEMS) have enabled the possibility of fabricating miniaturized sensors. Recently various types of MEMS force sensors have been reported for use in MIS with the purpose to provide force feedback [4]–[13]. Especially some are developed for guidewire/catheter related applications [14]–[18]. However, most of the reported force sensors that have been developed for MIS cannot be directly used in guidewire applications because of their incompatible mechanical structures. In this paper, a ring-shaped tri-axial force sensor to be mounted at the tip of a guidewire is reported. The developed sensor has a ring-shaped structure at the center that can be integrated on the distal tip of the guidewire by passing through the hollow core. Comparing with previous assembly arrangements reported in [13][19][20], the ring-shaped configuration is much simpler and easier to be integrated with circular shaped surgical tools. This assembly configuration minimizes the bending artifacts as it is directly integrated on the distal tip of the guidewire whereas most of the reported sensors developed for guidewire applications are mounted in a recess in the core wire. The output signal from the sensor is affected not only by the bending of the tip of guidewire itself but also the change in the physical environment surrounding the sensor [19].

II. SENSOR DESIGN

A. Sensor Design

The sensor design is inspired by the requirement of mounting a force sensor on the tip of a movable core guidewire to provide force feedback during catheterization procedures. Based on the core wire configuration at the distal end, standard commercial guidewires can be mainly divided into two different types, fixed core guidewire and movable core guidewire [21] as shown in Fig. 1.

Generally a guidewire comprises a distal tip, a core wire, a coil, and the cover. The fixed core guidewire has one single core wire from the proximal end to the distal tip of the guidewire which will enable direct torque transmission from proximal end to the tip. The moveable core guidewire has two separated core wires which is more flexible and steerable than the fixed core guidewire. The dimensions and other properties of the guidewires can vary considerably based on the type of procedure being performed and the anatomy of patients. In the conventional design, the outer diameter of the guidewire is ranged from 240 μm to 1mm whereas the core wire has a diameter ranged from 50 μm to 200 μm .

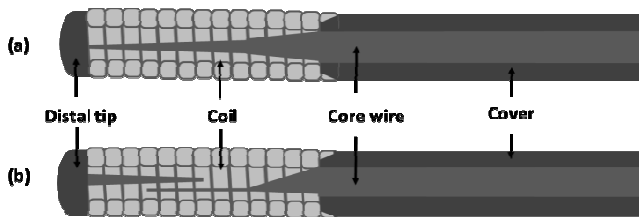


Fig. 1 Standard commercial guidewire designs, (a) fixed core guidewire (b) movable core guidewire

In order to be integrated on the tapered core wire on the distal end, the designed sensor should be of a small size less than 1 mm. The sensor must be capable of measuring forces in both normal and shear directions. High sensor resolution is also required to detect small changes in force and displacement with good linearity and low hysteresis. The designed sensor shall be integrated on the movable part of the core wire and located inside the coil. According to these requirements, a ring-shaped tri-axial force sensor has been designed as shown in Fig. 2.

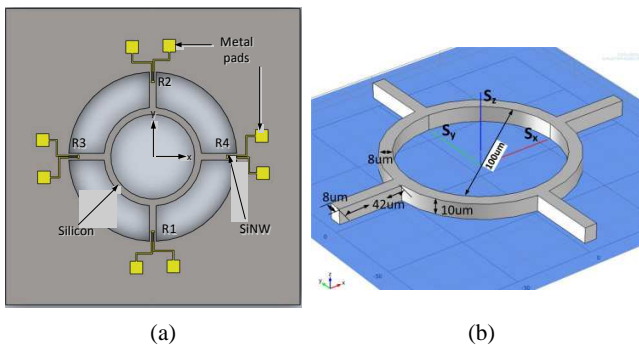


Fig. 2 (a) Schematic of the ring-shaped force sensor design (b) Dimensions of the sensor structure: beam 42 μm \times 8 μm \times 10 μm , inner ring diameter 100 μm , and outer ring diameter 116 μm

The designed sensor as shown in Fig. 2 (a) consists of a suspended ring-shaped structure located at the center and four suspended cantilever beams whose axes are perpendicular to each other. The movable tip of the core wire would pass through the ring structure to be integrated with the sensor and acts as a force transmission element. Single crystalline Silicon nanowires (SiNWs) are embedded at the end of each beam as piezoresistive sensing material because of its high gauge factor [22]. When an external force is applied on the structure, the ring deforms and the resistances of SiNWs change due to the induced strain.

The resistance changes can be measured by an additional electrical circuit. The dimensions of the sensor have been identified according to the structure dimension of guidewire where the force sensor is targeted to be integrated with. The overall dimension of the designed sensor should not exceed the inner diameter of the coil. The diameter of the inner ring should be larger than the diameter of the movable core wire. A finite element analysis was carried out to optimize the critical structural parameters of the sensor, such as the inner and outer diameter of the ring, and the cantilever length, width and thickness. Finally, as shown in Fig. 2 (b), the diameter of the inner ring is designed to be 100 μm and the diameter of the outer ring is designed to be 116 μm . The cantilever beam has a size of 42 μm \times 8 μm \times 10 μm in length, width, and thickness respectively. The sensing area including cantilever beams is 200 μm \times 200 μm whereas the total area of the sensor with metal pads is 400 μm \times 400 μm .

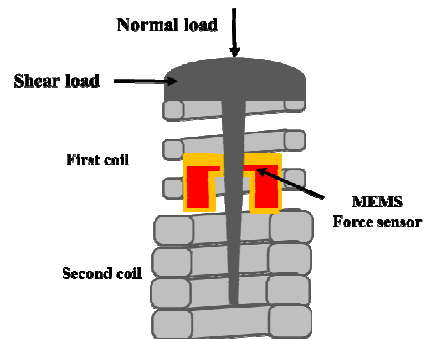


Fig. 3 Illustration of movable core guidewire with integrated MEMS force sensor

The integration scheme of the designed sensor and the movable core guidewire is illustrated in Fig. 3. A two coil structure has been designed with the purpose of inducing a differential displacement between the core wire and the coil to lead the ring deformation. The sensor is to be integrated with the movable core wire which is connected with the distal tip and located in the first coil. When external force applied at the end of the guidewire, displacement differences between the distal tip and the coil will induce a deformation of the sensor structure. The spring stiffness of the two coils can be appropriately designed to limit the displacement of the ring in a safety range such that the robustness of the sensor can be guaranteed.

B. Sensor Principle

When an external force is applied on the sensor, the structure is deformed and strain is induced. The relationship between the applied force and the ring displacement is as following:

$$F = K_e \Delta x \quad (1)$$

where F is the applied force, K_e is the equivalent spring stiffness of the sensor structure, and Δx is the ring displacement.

The piezoresistors change their resistance due to the ring displacement and the induced strain, which can be measured from the metal pads. The sensitivity of piezoresistors can be obtained by the following equation [24].

$$\frac{\Delta R}{R} = \pi_l \sigma_l + \pi_t \sigma_t \quad (2)$$

where R is the resistance without applied stress, ΔR is the resistance change with applied stress, π and σ represent the piezoresistive coefficient and stress respectively, and the subscripts l and t refer to longitudinal and transverse components.

Referring to Fig. of the labels of four piezoresistors, the sensitivity is defined as following.

$$\begin{aligned} S_x &= \left(\frac{\Delta R}{R}\right)_x = \frac{\Delta R_3}{R_3} - \frac{\Delta R_4}{R_4} \\ S_y &= \left(\frac{\Delta R}{R}\right)_y = \frac{\Delta R_1}{R_1} - \frac{\Delta R_2}{R_2} \\ S_z &= \left(\frac{\Delta R}{R}\right)_z = \frac{\Delta R_1}{R_1} + \frac{\Delta R_2}{R_2} + \frac{\Delta R_3}{R_3} + \frac{\Delta R_4}{R_4} \end{aligned} \quad (3)$$

where S_x, S_y, and S_z are the sensor sensitivities in the X-Y-Z directions respectively. When shear forces are applied, the opposite piezoresistors such as R1 and R2 will experience opposite strain (i.e. R1 will experience tensile strain whereas R2 will experience compressive strain, or vice versa). When normal loading is applied, the resistance of all four piezoresistors will have the same sign of strain (either tensile or compressive) and the Z axis sensitivity is defined as the total resistance change of all four piezoresistors.

III. FEM MODELING

A. FEM Modeling of Ring Sensor

A commercial finite element analysis tool, COMSOL, was used to study the mechanical behavior of the structure under various applied load conditions. The material properties used in the modeling were obtained from reported literature as shown in table 1.

In order to find the location of the maximum sensitivity to put the piezoresistors, regions of highest stress on the beams were identified by finite element modeling (FEM) as shown in Fig. When normal force is applied on the top surface of the ring, the sensor beams bend downward and the maximum stress is found at the bases of the beams. SiNWs are placed at these high stress regions to obtain maximum piezoresistance output. The maximum stress at the SiNWs must not exceed the yielding stress of single-crystalline silicon, the value of which is around 300 MPa. From the simulation, the applicable force range was found to be 0 to 5 mN to avoid fracture of the sensor. The load at the end of one cantilever beam is also analyzed. The stress field and simulated strain with a prescribed 1 μm displacement load D_z is presented in Fig. The load is applied at the junction area of a beam and the ring. The obtained stress and strain are linearly proportional to the applied load.

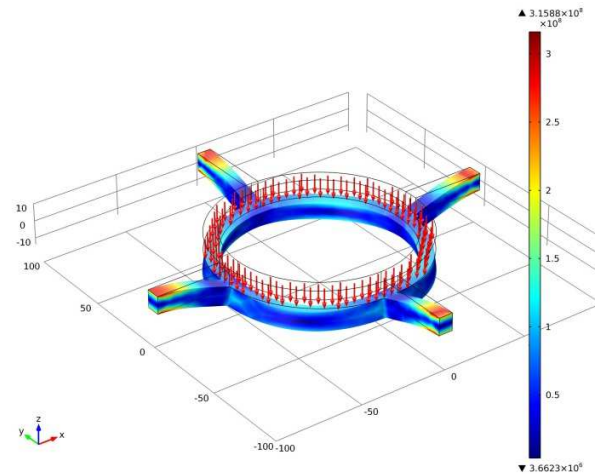


Fig. 4 COMSOL modeling result showing the von Mises stress field of the ring structure under 5mN force load applied in the z-direction.

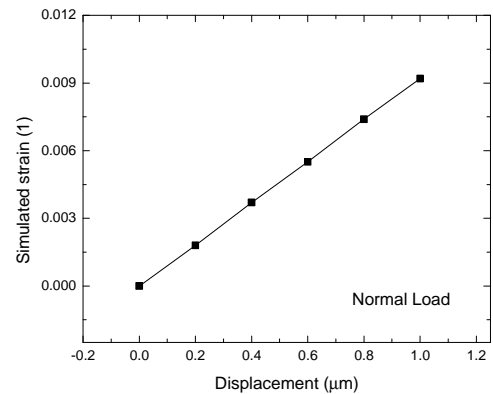
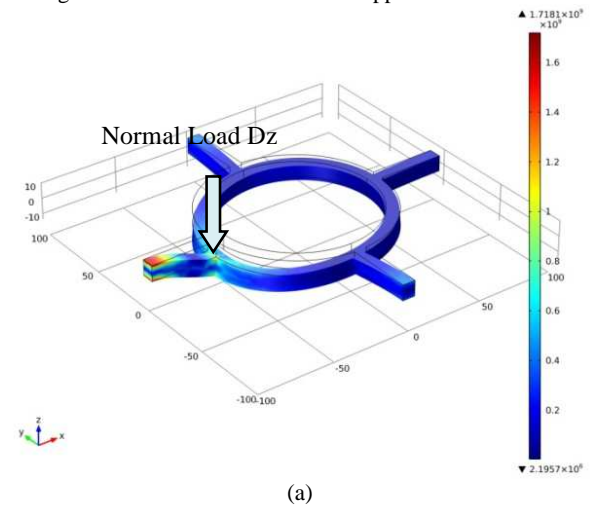


Fig. 5 (a) Von Mises stress field of the sensor in response to 1μm prescribed displacement loaded in the z direction. (b) Simulated strain versus displacement.

TABLE I
 MATERIAL PROPERTIES FOR MODELING

Material	Young's Modulus	Poisson Ratio	Density
Silicon	169GPa	0.278	2330 Kg/m ³
Steel	200GPa	0.33	7850 Kg/m ³
Epoxy	3.5GPa	0.069	1250 Kg/m ³

B. FEM Modeling of Sensor and Steel Wire Integration

The destination of the designed sensor is to be integrated on the distal tip of movable core guidewires to measure the normal and shear forces. An FEM modeling was done for the integration of the sensor and a steel wire. In this simulation, the steel wire passes through the ring and they are firmly integrated together by adhesive epoxy as shown in Fig. . The material properties are listed in table 1. The steel wire acts as force transmitting element when shear load applies. The stress field for normal and shear loads is presented in Fig. . During normal loading the lateral stress components in the four SiNWs are equal in magnitude with same direction as in Fig. 7 (a). When a transverse loading applied in the x- or y-direction, the two SiNWs along with the loading direction experience stress of the same magnitude but opposite signs. The other two SiNWs perpendicular to the loading undergo torsion as in Fig. 7 (b). A linear relationship was observed between the applied force on the steel wire and the induced stress on the SiNW as shown in Fig. 8.

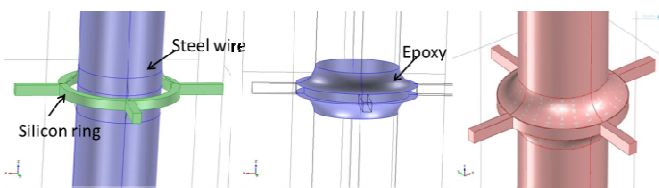


Fig. 6 Illustration of the steel wire integration with the ring sensor

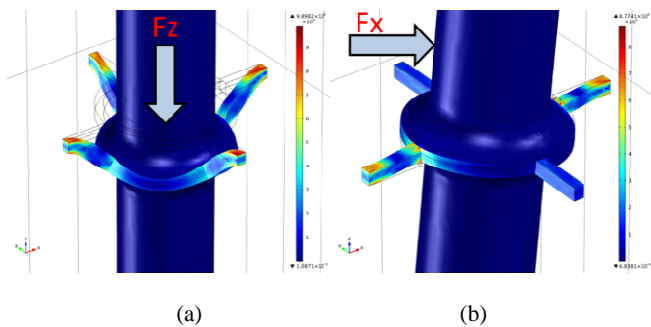


Fig. 7 Von Mises stress field of the steel wire integration on the ring sensor under normal (a) and shear load (b).

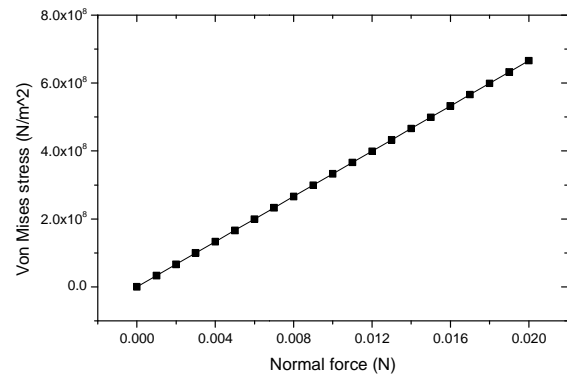


Fig. 8 Linear relationship between stress at the location of SiNW and the applied normal force on the steel wire

IV. CONCLUSION

A ring-shaped triaxial force sensor was designed and simulated according to the mechanical structure of the guidewire with the purpose of mounting at the distal tip of the movable core guidewires. The integration scheme of the sensor and guidewire has been presented that have a new designed guidewire tip structure comprising two coils at the distal end. The designed sensor comprises a ring-shaped structure located at the center of four cantilever beams. Piezoresistive SiNWs were used for sensing material to transform force to electric resistance. The sensor was designed and simulated using COMSOL, a commercial multiphysics simulation software, before the fabrication for stress analysis. Maximum stress location was found by FEM modeling. Mechanical behavior of the integration of the ring sensor and a steel guidewire was modeled and a linear relationship between applied load and the induced stress on the SiNWs was observed.

ACKNOWLEDGMENT

This work was funded by A*STAR science and research council under Grant 0921480070.

REFERENCES

- [1] G. S. Guthart and J. Salisbury, J.K., "The IntuitiveTM telesurgery system: overview and application", in Robotics and Automation, 2000. Proceedings. ICRA '00. IEEE International Conference on, 2000, vol. 1, pp. 618–621 vol.1.
- [2] A. J. Einstein, K. W. Moser, R. C. Thompson, M. D. Cerqueira, and M. J. Henzlova, "Radiation dose to patients from cardiac diagnostic imaging", *Circulation*, vol. 116, no. 11, pp. 1290–1305, Nov 2007.
- [3] R. Razavi, D. L. Hill, S. F. Keevil, M. E. Miquel, V. Muthurangu, S. Hegde, K. Rhode, M. Barnett, J. van Vaals, D. J. Hawkes, and E. Baker, "Cardiac catheterisation guided by MRI in children and adults with congenital heart disease", *The Lancet*, vol. 362, no. 9399, pp. 1877–1882, 2003.
- [4] Yating Hu, R. B. Katragadda, Hongen Tu, Qinglong Zheng, Yuefa Li, and Yong Xu, "Bioinspired 3-D tactile sensor for minimally invasive surgery", *Microelectromechanical Systems*, *Journal of*, vol. 19, no. 6, pp. 1400–1408, 2010.
- [5] J. Dargahi, M. Parameswaran, and S. Payandeh, "A micromachined piezoelectric tactile sensor for an endoscopic grasper-theory, fabrication and experiments", *Journal of Microelectromechanical Systems*, vol. 9, no. 3, pp. 329–335, Sep 2000.
- [6] J. Peirs, J. Clijnen, D. Reynaerts, H. V. Brussel, P. Herijgers, B. Corneville, and S. Boone, "A micro optical force sensor for force feedback

- during minimally invasive robotic surgery”, *Sensors and Actuators A: Physical*, vol. 115, no. 2–3, pp. 447–455, Sep 2004.
- [7] P. Valdastrì, K. Harada, A. Menciassi, L. Beccai, C. Stefanini, M. Fujie, and P. Dario, “Integration of a miniaturized triaxial force sensor in a minimally invasive surgical tool”, *Biomedical Engineering, IEEE Transactions on*, vol. 53, no. 11, pp. 2397–2400, Nov 2006.
- [8] P. Puangmali, H. Liu, L. D. Seneviratne, P. Dasgupta, and K. Althoefer, “Miniature 3-axis distal force sensor for minimally invasive surgical palpation”, *IEEE/ASME Transactions on Mechatronics*, vol. PP, no. 99, pp. 1–11, 0.
- [9] P. Puangmali, K. Althoefer, L. D. Seneviratne, D. Murphy, and P. Dasgupta, “State-of-the-art in force and tactile sensing for minimally invasive surgery”, *Sensors Journal, IEEE*, vol. 8, no. 4, pp. 371–381, 2008.
- [10] A. L. Trejos, R. V. Patel, and M. D. Naish, “Force sensing and its application in minimally invasive surgery and therapy: a survey”, *Proceedings of the Institution of Mechanical Engineers, Part C: Journal of Mechanical Engineering Science*, vol. 224, no. 7, pp. 1435–1454, Jan 2010.
- [11] S. Sokhanvar, M. Packirisamy, and J. Dargahi, “MEMS endoscopic tactile sensor: toward in-situ and in-vivo tissue softness characterization”, *Sensors Journal, IEEE*, vol. 9, no. 12, pp. 1679–1687, 2009.
- [12] P. Peng, A. S. Sezen, R. Rajamani, and A. G. Erdman, “Novel MEMS stiffness sensor for in-vivo tissue characterization measurement”, in *Engineering in Medicine and Biology Society, 2009. EMBC 2009. Annual International Conference of the IEEE*, 2009, pp. 6640–6643.
- [13] M. A. Qasaimeh, S. Sokhanvar, J. Dargahi, and M. Kahrizi, “PVDF-based microfabricated tactile sensor for minimally invasive surgery”, *Microelectromechanical Systems, Journal of*, vol. 18, no. 1, pp. 195–207, 2009.
- [14] H.-L. Chau and K. D. Wise, “An ultraminiature solid-state pressure sensor for a cardiovascular catheter”, *Electron Devices, IEEE Transactions on*, vol. 35, no. 12, pp. 2355–2362, 1988.
- [15] M. Esashi, H. Komatsu, T. Matsuo, M. Takahashi, T. Takishima, K. Imabayashi, and H. Ozawa, “Fabrication of catheter-tip and sidewall miniature pressure sensors”, *Electron Devices, IEEE Transactions on*, vol. 29, no. 1, pp. 57–63, 1982.
- [16] P. Polygerinos, D. Zbyszewski, T. Schaeffter, R. Razavi, L. D. Seneviratne, and K. Althoefer, “MRI-compatible fiber-optic force sensors for catheterization procedures”, *Sensors Journal, IEEE*, vol. 10, no. 10, pp. 1598–1608, Oct 2010.
- [17] C. Li, P.-M. Wu, J. Han, and C. Ahn, “A flexible polymer tube lab-chip integrated with microsensors for smart microcatheter”, *Biomedical Microdevices*, vol. 10, no. 5, pp. 671–679, 2008.
- [18] T. Meiß, T. A. Kern, S. Sindlinger, and R. Werthschützky, “HapCath: highly miniaturized piezoresistive force sensors for interior palpation of vessels during angioplasty”, in *World Congress on Medical Physics and Biomedical Engineering, September 7 - 12, 2009, Munich, Germany*, vol. 25/6, O. Dössel and W. C. Schlegel, Eds. Berlin, Heidelberg: Springer Berlin Heidelberg, 2009, pp. 228–231.
- [19] O. Hammarström, P. Benkowski, P. von Malmborg, and L. Tenerz, “Sensor and guide wire assembly”, U.S. Patent 633690608-Jan-2002.
- [20] L. Tenerz and L. Smith, “Sensor and guide wire assembly”, U.S. Patent 734381118-Mar-2008.
- [21] I.-I. O. for Standardization, “ISO - International Organization for Standardization”. [Online]. Available: http://www.iso.org/iso/iso_catalogue/catalogue_tc/catalogue_detail.htm?csnumber=19052. [Accessed: 24-Jun-2012].
- [22] P. Neuzil, C. C. Wong, and J. Reboud, “Electrically controlled giant piezoresistance in silicon nanowires”, *Nano Lett.*, vol. 10, no. 4, pp. 1248–1252, 2010.
- [23] L. Lou, K. Ramakrishna, L. Shao, W.-T. Park, D. Yu, L. Lim, Y. Wee, V. Kripesh, H. Feng, B. S. Y. Chua, C. Lee, and D.-L. Kwong, “Sensorized guidewires with MEMS tri-axial force sensor for minimally invasive surgical applications”, in *Engineering in Medicine and Biology Society (EMBC), 2010 Annual International Conference of the IEEE*, 2010, pp. 6461–6464.
- [24] S. D. Senturia, *Microsystem Design*. Springer, 2001.